THE JOURNAL OF BIOLOGICAL CHEMISTRY VOL. 287, NO. 28, pp. 23594–23603, July 6, 2012

A Viral Deubiquitylating Enzyme Restores Dislocation of Substrates from the Endoplasmic Reticulum (ER) in Semi-intact Cells*

Received for publication, March 22, 2012, and in revised form, May 2, 2012 Published, JBC Papers in Press, May 22, 2012, DOI 10.1074/jbc.M112.365312

Sumana Sanyal[‡], **Jasper H. L. Claessen**[‡1], **and Hidde L. Ploegh**[‡§2]

From the [‡]*Whitehead Institute for Biomedical Research and the* [§]*Department of Biology, Massachusetts Institute of Technology, Cambridge, Massachusetts 02142*

Background: Substrate dislocation to the cytosol is a key step in the process of ER quality control.
Results: Exogenous addition of a deubiquitylating enzyme to semi-intact cells restores dislocation of stalled intermediates.
Conclusion: Substrates undergo two rounds of ubiquitylation prior to proteasomal degradation.
Significance: This study provides a key mechanistic insight in the dislocation reaction that clears misfolded substrates from the ER.

Terminally misfolded glycoproteins are ejected from the endoplasmic reticulum (ER) to the cytosol and are destroyed by the ubiquitin proteasome system. A dominant negative version of the deubiquitylating enzyme Yod1 (Yod1C160S) causes accumulation of dislocation substrates in the ER. Failure to remove ubiquitin from the dislocation substrate might therefore stall the reaction at the exit site from the ER. We hypothesized that addition of a promiscuous deubiquitylase should overcome this blockade and restore dislocation. We monitored ER-to-cytosol transport of misfolded proteins in cells permeabilized at high cell density by perfringolysin O, a pore-forming cytolysin. This method allows ready access of otherwise impermeant reagents to the intracellular milieu with minimal dilution of cytoplasmic components. We show that addition of the purified Epstein-Barr virus deubiquitylase to semi-intact cells indeed initiates dislocation of a stalled substrate intermediate, resulting in stabilization of substrates in the cytosol. Our data provide new mechanistic insight in the dislocation reaction and support a model where failure to deubiquitylate an ER-resident protein occludes the dislocon and causes upstream misfolded intermediates to accumulate.

Protein transport across the ER[3] encompasses reactions on both the cytoplasmic and luminal side of the ER membrane. Although we understand in considerable detail the structure and *modus operandi* of the components necessary for co-translational transport of nascent polypeptides through the translocon (1), much remains to be learned about the reverse process, *i.e.* protein transport from the ER to the cytoplasm *en route* to degradation by the ubiquitin-proteasome system (UPS). In eukaryotic cells, a fraction of newly synthesized proteins misfolds early during their biogenesis and is degraded. Efficient disposal of defective proteins is essential, because these proteins, even if only partially folded, may compete with their functional counterparts for substrate binding or for complex formation with interaction partners and so exert a dominant negative effect (2). Defective secretory and transmembrane proteins likewise present an inherent risk; if released from the cell or exposed at the cell surface, they could interfere with function. Eukaryotic cells therefore must exert stringent quality control over secretory proteins, initiated at their site of synthesis.

Terminally misfolded proteins in the ER are recognized and targeted for disposal, mostly in the cytosol. How such proteins traverse the ER membrane to reach the cytosol remains to be established. Several proteins, including the Hrd1 E3-ligase (3), Sec61, and members of the Derlin family of proteins, have been proposed to form a dislocation channel (4–6) to facilitate export of misfolded substrates across the ER. Alternative nonconventional modes of transport across the ER bilayer have been suggested (7) and challenged (8). Multiple strategies presumably exist in mammalian cells to facilitate substrate passage into the cytosol, depending on specificity and physical characteristics of the substrates, but currently known pathways mostly converge on degradation by the UPS. How exactly the initial encounter with an appropriate E3 ligase(s) occurs is easily envisioned for an ER-resident protein that spans the membrane and has at least a portion exposed to the cytosolic ubiquitylation machinery, but how a completely luminal degradation substrate engages its cognate Ub ligase(s) is less apparent. Auxiliaries that recognize the misfolded state in the ER lumen presumably direct degradation substrates to the appropriate location (9, 10). A cascade of E1, E2, and E3 activities catalyzes ubiquitylation, a reaction that can be reversed by ubiquitin-specific proteases, of which there are many (11).

The analysis of the mammalian Hrd1-Sel1L ubiquitin E3 ligase complex has uncovered a complex set of functionally

* This work was supported, in whole or in part, by National Institutes of Health Grants (to H. L. P.).
[1] Fellow of the Boehringer Ingelheim Fonds.
[2] To whom correspondence should be addressed: Whitehead Institute for Biomedical Research, Nine Cambridge Center, Dept. of Biology, Massachusetts Institute of Technology, Cambridge, MA 02142. Tel.: 617-324-2031; Fax: 617-452-3566; E-mail: ploegh@wi.mit.edu.
[3] The abbreviations used are: ER, endoplasmic reticulum; DUB, deubiquitylating enzyme; EBV, Epstein-Barr virus; PFO, perfringolysin O; HCMV, human cytomegalovirus; UPS, ubiquitin-proteosome system; Ub, ubiquitin; HBSS, Hanks' balanced salt solution; GTPγS, guanosine 5′-3-*O*-(thio)triphosphate; ATPγS, adenosine 5′-*O*-(thiotriphosphate); TCRα, T-cell receptor α; PDI, protein-disulfide isomerase.

important interactors that act downstream of ubiquitylation. Prominent among which is the AAA-ATPase p97, and in turn, via p97, an even more expansive set of interactors (9, 12). Although the role of some proteins in this pathway is clear, the involvement of others is either controversial or lacks experimental support. The confusing and somewhat contradictory data on the involvement of specific proteins reflects the technical challenges, notably the lack of robust *in vitro* systems, inherent in current approaches to study dislocation.

The ubiquitin-specific protease Yod1 plays a role in clearing the ER of several misfolded substrates (13, 14). Expression of a dominant negative version of Yod1 (the YodC160S mutant, which lacks catalytic activity) leads to accumulation in the ER of substrates (in their nonubiquitylated state) that would otherwise have been discharged and destroyed (13). We hypothesized that a failure to remove ubiquitin from a dislocation substrate *en route* from the dislocon to the next station in the dislocation pathway would stall the substrate and block all further dislocation. We exploited the activity of an Epstein-Barr virus-derived ubiquitin-specific protease domain, excised from its normal sequence context and expressed as the isolated active domain (EBV-DUB) to interfere with ubiquitin-dependent events in protein quality control (15). To overcome the block imposed by Yod1C160S, we proposed that expression of EBV-DUB protease would remove Ub from substrates targeted for degradation and stabilize them either at the ER membrane or in the cytosol (15). Expression of EBV-DUB indeed caused an enzymatic blockade of the UPS and resulted in accumulation in the cytosol of intermediates and in the lumen of the ER that would otherwise have been destroyed. The ubiquitylation events that determine extraction from the ER are thus separable from ubiquitylation reactions that target a substrate for proteasomal degradation (Fig. 1).

Occlusion of the dislocon by ubiquitylated intermediates and concomitant trapping of other substrates in the ER could account for the effects of expression of dominant negative Yod1, but formal proof for the suggestion is lacking. Alternatively, both the expression of dominant negative Yod1, of EBV-DUB, or the combination of the two might set in motion a program of gene expression that fundamentally alters the molecular composition of the ER and the dislocation machinery. With the above unsolved questions in mind, we have developed an *in vitro* assay to test the proposed model that stipulates two cycles of ubiquitylation and deubiquitylation to arrive at recognition, extraction, and disposal of an ER luminal misfolded protein (9).

Here, we test the role of deubiquitylation in this model using an *in vitro* dislocation assay performed in semi-intact cells. The configuration of this assay not only allows us to avoid dilution of cytoplasmic components, it also enables manipulation, within certain limits, of the composition of the cytoplasmic environment through osmotic delivery of small molecules and proteins, including active and inactive versions of enzymes such as EBV-DUB or trypsin, as well as ATP and GTP analogs. To establish unambiguously the effect of EBV-DUB on cells that express the catalytically inactive Yod1, we created semi-intact cells through treatment with perfringolysin O (PFO), a cholesterol-binding pore-forming toxin. We delivered purified EBV to the cytoplasm of these semi-intact cells by administration of a transient hypotonic shock, and so directly explored the role of deubiquitylation in the transport of misfolded proteins. Delivery of exogenous EBV-DUB to semi-intact cells loaded with a stalled dislocation substrate released such intermediates from the ER and jump-started delivery to the cytoplasm. Our results provide a new mechanistic insight and direct proof of a key feature of the proposed mechanism of dislocation. Because delivery of exogenous cytosol supports substrate dislocation in semi-intact cells, it should be possible to identify specific cytosolic components that are essential to this process.

EXPERIMENTAL PROCEDURES

Antibodies, Cell Lines, Constructs—Antibodies against the HA epitope were purchased from Roche Applied Science (3F-10). Polyclonal anti-PDI serum (rabbit) was generated with bacterially expressed human PDI, and anti-BiP serum (rabbit) was against human BiP. Antibodies against GAPDH and p97 were purchased from Abcam. TCRα antibody has been described before (15, 16). ATPγS and GTPγS were purchased from Sigma. HEK293T cells were purchased from American Type Culture Collection and cultured. US11 cell lines have been described (12, 13). The construct containing EBV-DUB has been described before (15, 17). For purification, the gene encoding EBV-DUB was modified to include a histidine tag, cloned into an expression vector, and overexpressed and purified from BL-21 competent *Escherichia coli*. Deletion constructs of ribophorin (RI_{332}) and the dominant negative mutant construct of YOD1 have been described elsewhere (13). HA-agarose beads were purchased from Roche Applied Science, and protein A-agarose beads were from RepliGen Bioprocessing.

Transient Transfections and Viral Transductions—HEK293T cells were transiently transfected using FuGENE 6 (Roche Diagnostics) according to the manufacturer's instructions. Cell transduced with pLHCX-based vectors (Clontech) were selected and maintained in 125 μg/ml of hygromycin B (Roche Applied Science).

Overexpression and Purification of His_6-PFO(C459A)—The gene encoding PFO from *Clostridium perfringens* was modified to replace the single cysteine with alanine (C459A) and include a NH_2-terminal hexahistidine tag (14, 17). This construct was subsequently cloned into the pRSETB expression vector (Invitrogen) and was kindly provided to us by A. Johnson (Texas A&M, College Station, TX). After transformation into BL21 *E. coli* competent cells, overexpression and purification were carried out using routine nickel-nitrilotriacetic acid affinity purification. The hexahistidine tag and the single amino acid substitution do not significantly affect the cholesterol binding activity of PFO as described (17).

Pulse-Chase Analysis, Immunoprecipitation, SDS-PAGE, and Intact Cells—Pulse-chase experiments were performed as described previously (14, 18). Briefly, $\sim 1 \times 10^7$ cells were detached by trypsinization and starved for 45 min in methionine/cysteine-free Dulbecco's modified Eagle's medium at 37 °C prior to pulse labeling. Cells were labeled for 10 min at 37 °C with 10 mCi/ml [^{35}S]methionine/cysteine (expressed protein mix; PerkinElmer Life Sciences) and chased for the

indicated time intervals. At appropriate time intervals, aliquots were withdrawn and treated with 0.1 μM PFO as described below. Immunoprecipitations were performed for at least 3 h at 4 °C with gentle agitation. Samples were eluted by boiling in reducing sample buffer, subjected to SDS-PAGE, and visualized by autoradiography.

PFO-mediated Permeabilization of Intact Cells—~1 × 10^7 cells were detached from 10-cm dishes by brief trypsinization, washed once with Hanks' balanced salt solution (HBSS), and resuspended in 50 μl of HBSS on ice. 50 μM of 200 nM PFO was added to a suspension of cells maintained on ice to obtain a final concentration of 100 nM. Excess PFO (unbound to the plasma membrane) was removed by diluting with 1 ml of HBSS and centrifugation (5 min; 500 × *g*). Cell pellets were resuspended in 50 μl of HBSS and incubated at 37 °C for 10 min. Following permeabilization, cells were centrifuged at 500 × *g* for 5 min to collect supernatants. Pellets obtained were washed once with 1 ml of HBSS and resuspended in 50 μl of HBSS containing 1% SDS. Separation of the cytosol and the organelle fractions was verified by immunoblotting for GAPDH, p97 (as cytosolic markers), BiP, and PDI (as soluble ER luminal markers).

Add-back Assays in PFO-permeabilized Cells—Cells transfected with either RI_{332} or TCRα were grown to 80–90% confluency and metabolically labeled with [^{35}S]cysteine/methionine at 37 °C in suspension. To create semi-intact cells for add-back of purified EBV, cells were treated with 0.1 μM PFO (in HBSS) on ice as described above. Excess PFO was removed by diluting in HBSS and centrifugation. For measuring substrate dislocation in semi-intact cells, the reaction mixture consisted of ~0.5 × 10^7 PFO-treated cells, 1 mM ATP, 40 μg of concentrated cytosol, and 10 μg of purified EBV resuspended in 50 μl of 0.5× HBSS and was incubated at 37 °C for appropriate time intervals. At each time point, withdrawn cell suspension was centrifuged at 500 × *g* for 5 min to separate the pellet and supernatant fractions. The pellet was lysed in Nonidet P-40 containing 0.1% SDS. The supernatants were diluted to 1 ml in Nonidet P-40 lysis buffer containing 0.1% SDS. Substrates were recovered from supernatant and pellet fractions by immunoprecipitation, resolved by SDS-PAGE, and visualized by autoradiography.

Preparation of Cytosol from HEK293T Cells—To prepare concentrated cytosol, HEK293T cells were grown in 15-cm dishes to confluency and harvested by brief trypsinization. Harvested cells were resuspended in 100 μl of Hanks' buffer and treated with 100 nM PFO on ice. Excess unbound PFO was removed by diluting with excess Hanks' buffer, centrifuging (500 × *g*), and resuspended in 20 μl of Hanks' buffer to introduce minimal dilution of cytosolic components. The cell suspension was then incubated at 37 °C for 10 min to induce pore formation by PFO. The supernatant (~100 μl) was collected after a 10,000 × *g* spin, measured for protein concentration, and immunoblotted for cytosolic and soluble ER luminal marker proteins. Cytosol concentration typically varied between 10 and 20 mg/ml. Concentrated cytosol was aliquoted into a 50-μl volume, flash-frozen in liquid nitrogen, and stored at −80 °C for later use.

RESULTS

PFO-mediated Selective Permeabilization of the Plasma Membrane—ER protein quality control entails recognition of terminally misfolded proteins through interaction of chaperones, lectins, and co-factors (9, 10). Substrates are then targeted to the dislocon, a putative channel of unknown composition, presumably as partially unfolded intermediates. These intermediates undergo a round of ubiquitylation by the Hrd1 E3 ligase complex (or another appropriate E3 ligase complex) for recruitment of downstream dislocation components (p97-Npl4-Ufd1) and subsequent de-ubiquitylation for passage through the p97 hexameric complex (9). Expression of a dominant negative variant of Yod1 (Yod1C160S), a deubiquitylating enzyme, arrests misfolded substrates in the ER lumen (13) implying that at least a fraction of the accumulated substrate intermediates at the ER membrane must be ubiquitylated. We propose that once in the cytosol, substrates must undergo a second round of ubiquitylation to engage the proteasome complex. *N*-Glycanase acts on glycoprotein substrates to remove attached *N*-linked glycan moieties, a reaction apparently dispensable for degradation (19), but experimentally quite informative because of the telltale reaction products that are diagnostic for dislocation. Deglycosylated polyubiquitylated substrates are then targeted to the proteasome and degraded (Fig. 1).

Experimental analyses of dislocation have been confounded by the intrinsic properties of the ER membrane, which is easily disrupted by the commonly used homogenization techniques or upon detergent solubilization. Measurements of protein transport from the ER requires a more intact ER structure than is provided by standard homogenization protocols. To this end, we devised a PFO-based method (20) of preparing semi-intact cells to monitor protein dislocation, modified by performing the permeabilization step in a minimal volume at high cell density (Fig. 1*B*). We hypothesized that supplying purified EBV-DUB in the presence of concentrated cytosol to semi-intact cells that harbor a block in dislocation due to Yod1C160S should overcome this barrier and release substrates from the ER to the cytosol. The method of creating semi-intact cells through mechanical shearing (21–23) or treatment with streptolysin O (20, 21, 23) is well documented and has been successfully used in the past to reconstitute protein transport through the secretory pathway. PFO is a member of the cholesterol-binding family of bacterial toxins. After binding to the plasma membrane, PFO monomers diffuse laterally in the plane of the bilayer and interact as homotypic aggregates that form large transmembrane pores (diameter ~25 nm (20, 21, 23, 24)). Although PFO binds to the plasma membrane at 0 °C, perforation requires exposure of PFO-treated cells to 37 °C. To assay dislocation, we exploit this pore-forming property of PFO (Fig. 2*A*). Confluent HEK293T cells (~1 × 10^7) are harvested by brief trypsinization, washed once with HBSS, resuspended in 50 μl of HBSS, and maintained on ice. 50 μl of 0.2 μM PFO (in HBSS) is added to the cell suspension and incubated on ice for 5 min to allow binding of the toxin to cholesterol at the plasma membrane without perforating the cells. Excess unbound PFO is then removed by diluting to 1 ml and centrifuging (500 × *g* for 5 min at 4 °C), followed by incubation of the cell suspension in a minimal vol-

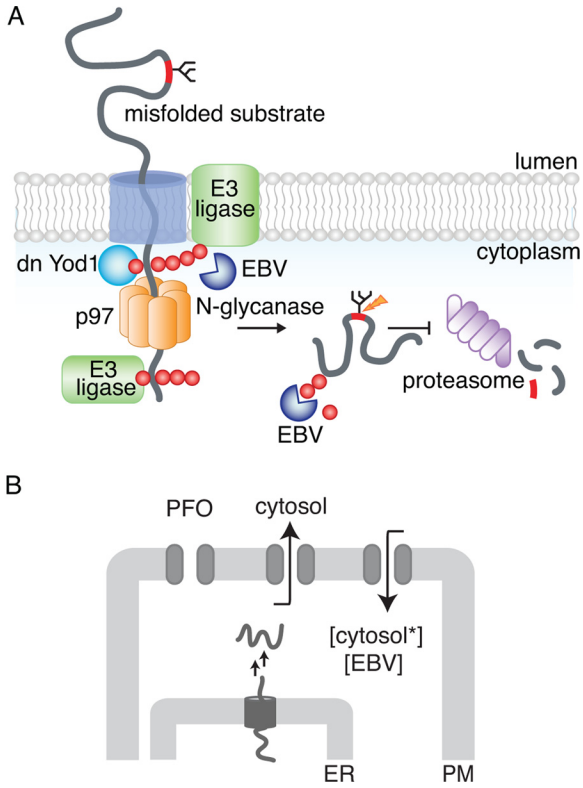

FIGURE 1. **Intracellular protein degradation by the ubiquitin proteasome system.** *A,* model for misfolded protein transport from the ER to the cytosol. A terminally misfolded glycoprotein is recognized by luminal chaperones and targeted to a putative channel in the membrane. The partially unfolded substrate is dislocated across the ER bilayer where ubiquitylation occurs through membrane-bound ubiquitin ligases, facilitating recruitment of p97. Deubiquitylation by Yod1 facilitates substrate transport through the hexameric AAA-ATPase to reach the cytosol where a second round of ubiquitylation presumably occurs. As depicted in the figure, expression of a dominant negative Yod1 (Yod1C160S) arrests polyubiquitylated substrates at the ER membrane. Cytosolic *N*-glycanase removes the glycan moiety from the substrate, prior to proteasomal degradation. In the presence of soluble EBV-DUB, polyubiquitin chains are removed from the substrate either at the ER membrane or in the cytosol and stabilized. *B, in vitro* assay to monitor protein dislocation from the ER to the cytosol in semi-intact cells. Cells with their plasma membrane (*PM*) selectively permeabilized are incubated with concentrated cytosol (*cytosol**) and EBV. If deubiquitylation is required for dislocation, addition of EBV to cells with substrates arrested in the ER should resume dislocation from the ER to the cytosol.

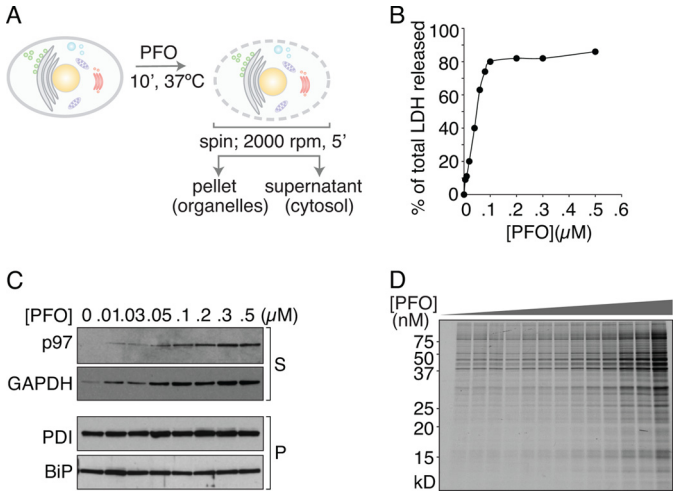

FIGURE 2. **Characterization of PFO-mediated cell permeabilization.** *A,* schematic of perfringolysin O-mediated semi-intact cell preparation. Adherent cells in culture are trypsinized to bring into suspension and treated with 100 nM PFO on ice. Excess unbound PFO is removed by diluting to 1.0 ml, centrifuged (500 × *g*, 5 min, 4 °C), and incubated at 37 °C after resuspension in 50 μl (1× HBSS) to induce pore formation. After the indicated time intervals, the reaction mixture was centrifuged (500 × *g*, 5 min, 4 °C) to separate supernatant and pellet fractions, which consist of the cytosol and organelles, respectively. *B,* supernatant fractions collected from PFO-treated cells were tested for release of cytosolic lactate dehydrogenase activity with increasing concentrations of PFO. *C,* supernatant and pellet fractions were probed for cytosolic and ER luminal marker proteins by immunoblotting to verify proper separation. GAPDH and p97 were measured in the cytosolic fraction; BiP and PDI were used as ER luminal markers and measured in the pellet fractions. As shown, with increasing concentrations of PFO used for permeabilization, the amount of GAPDH and p97 released increases, suggestive of a higher number of pores formed at the plasma membrane. BiP and PDI in the pellet fractions remain constant under all conditions, indicating that the ER integrity is maintained at the PFO concentrations used. *D,* [^{35}S]cysteine/methionine-labeled cells were subjected to permeabilization with varying PFO concentrations (0, 5, 10, 20, 25, 30, 40, 50, 75, 100, 200, 300, 400, and 500 nM). The supernatants collected were visualized by autoradiography to measure size distribution of materials released from cells as a function of PFO concentration. All experiments were performed at least twice.

ume of 50 μl at 37 °C for 10 min to initiate pore formation. Supernatant and pellet fractions were then separated by mild centrifugation for 5 min at 500 × *g*. The supernatant fraction contains cytosolic proteins as shown by the dose-dependent increase in released lactate dehydrogenase activity (Fig. 2*B*). In addition, the amount of cytosolic GAPDH and p97, enzymes of cytosolic disposition, appear in the supernatant with increasing concentrations of PFO as observed by immunoblotting (Fig. 2*C*). The levels of ER-luminal soluble proteins PDI and BiP remain unchanged in the pellet fraction over this concentration range of PFO, indicating that integrity of the ER membrane is retained. Analysis by SDS-PAGE of the supernatant fraction obtained at different PFO concentrations shows a size distribution of released [^{35}S]cysteine/methionine materials that is independent of PFO concentration, whereas the amount of materials released increases as the PFO concentration is raised (Fig. 2*D*). This observation suggests that the number of pores, but not their size, is a function of PFO concentration. The rate of pore formation is rapid; a time course of the release of cytosolic contents upon treatment with 0.1 μM PFO reaches a plateau within ~10 min, and the size of the pores formed is sufficient to allow passage of proteins as large as ~200 kDa (Fig. 2*D*). Cells treated with PFO remain functional in many respects, which is evident from the protein trafficking events along the secretory pathway in semi-intact cells, as measured by glycan maturation of vesicular stomatitis virus glycoprotein (VSV-G). Kinetics of VSV-G trafficking from the ER to the Golgi in semi-intact cells supplemented with ATP and cytosol was monitored by its acquisition of complex-type *N*-linked glycans, as assessed by digestion of VSV-G with endoglycosidase H. Samples of VSV-G recovered from PFO-treated and intact cells were identical in this regard. As described below, glycan maturation was blocked in semi-intact cells upon inclusion of nonhydrolysable NTP analogs GTPγS and ATPγS, which are without effect in intact cells, demonstrating access to the cytosol of cell-impermeant compounds to perforation by PFO. Similarly, in influenza-infected cells, we monitored maturation of neuraminidase, a type II membrane glycoprotein and hemagglutinin, and we observed no

differences in the rates of complex *N*-linked glycan acquisition for intact and PFO-treated semi-intact cells.[4]

Substrate Dislocation Measured in Semi-intact Cells, Appearance of a Trypsin-sensitive Deglycosylated Intermediate of RI_{332}—We tested our assay strategy (see schematic in Fig. 1*B*) in HEK293T cells expressing either Yod1C160S or EBV-DUB, starting with a set of substrates commonly used as model misfolded proteins, including both soluble and membrane proteins. As reporters, we used a truncated version of ribophorin (RI_{332}; soluble), T-cell receptor α subunit (type I membrane protein), and class I MHC molecules (type I membrane protein) in U373 cells that express the US11 immunoevasin from HCMV as reporters (18).

RI_{332} is a glycoprotein, the majority of which carries a single *N*-linked glycan, with a minor fraction never receiving its glycan (nonglycosylated) in the ER (15, 25). Once exported from the ER to the cytosol, the *N*-linked glycan is removed by cytosolic *N*-glycanase, resulting in a shift in electrophoretic mobility distinct from that of the nonglycosylated form of RI_{332}. To measure dislocation in semi-intact cells, we treated HEK293T cells that express RI_{332} with 0.1 μM PFO and incubated them with concentrated cytosol supplemented with ATP at 37 °C. At the indicated time intervals, we separated the pellet and supernatant fractions to probe for RI_{332} by immunoprecipitation. In cells expressing only RI_{332}, we observed time-dependent proteasomal degradation (Fig. 3*A*, *3rd* and *4th lanes*) of RI_{332}, tightly coupled to its export from the ER. Therefore, RI_{332} is not detected in the supernatant (cytosolic) fractions in the absence of proteasome inhibitors. In cells transfected with Yod1C160S, all RI_{332} remains in the ER lumen due to blocked dislocation (13), and hence we find RI_{332} in the pellet fraction in its glycosylated form (Fig. 3*A*, *5th to 8th lanes*). In contrast, co-transfection with EBV-DUB stabilizes RI_{332} in either one of two stages (15); a fraction of RI_{332} was arrested in the ER membrane due to removal of ubiquitin required for substrate engagement by p97-Ufd1-Npl4. The fraction dislocated into the cytosol is deglycosylated, but not degraded, because the cytosolic fraction of RI_{332} lacks the polyubiquitin tag essential for proteasomal degradation (15). Indeed, deglycosylated RI_{332} appears in the cytosol at 90 min (Fig. 3*A*, *9th to 12th lanes*). The accumulation of the deglycosylated intermediate is similar to what we observe when proteasomal activity is impaired by chemical inhibitors such as Zl_3VS (16, 26).

Is the fraction of deglycosylated RI_{332} indeed cytosolically oriented? If PFO treatment compromises plasma membrane integrity without permeabilizing the ER, de-glycosylated cytosolic RI_{332} should be trypsin-sensitive, whereas fully glycosylated, luminally oriented RI_{332} should remain protected. We prepared semi-intact cells and added purified trypsin via a mild hypotonic shock (see below) to measure protease sensitivity of RI_{332}. As observed with microsome preparations (15), added trypsin destroyed the deglycosylated version of RI_{332} without attacking the fully glycosylated form (Fig. 3*A*, *13th to 16th lanes*); trypsin added after pretreatment with a trypsin inhibitor did not proteolyze deglycosylated RI_{332}, as expected (Fig. 3*A*, *17th to 20th lanes*).

[4] S. Sanyal, and H. L. Ploegh, unpublished observations.

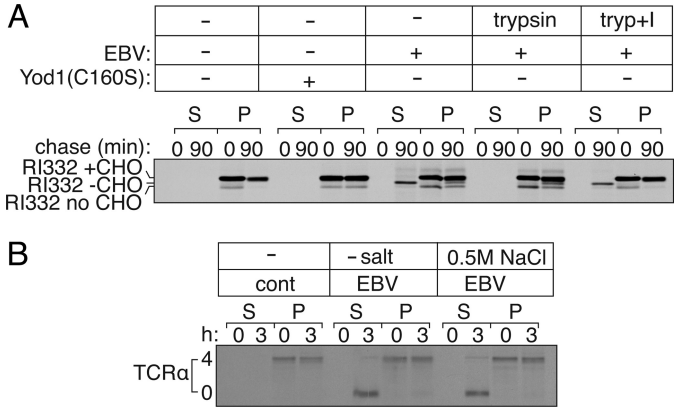

FIGURE 3. **Misfolded protein dislocation measured in semi-intact cells.** *A,* HEK293T cells were transiently transfected with RI_{332} and either Yod1 (C160S) or EBV. Cells were pulse-labeled for 10 min with [^{35}S]cysteine/methionine, permeabilized using PFO, and chased for 90 min in Hanks' buffer supplemented with 40 μg of cytosol prepared separately and 1 mM ATP. At 0- and 90-min time points, semi-intact cells were centrifuged at 500 $\times$ *g* for 5 min at 4 °C to separate supernatant (*S*) and pellet (*P*) fractions; RI_{332} was immunoprecipitated from all fractions and resolved by autoradiography. In the absence of Yod1(C160S) or EBV, RI_{332} is degraded in semi-intact cells with kinetics similar to that observed in intact cells (*1st to 4th lanes*). In the presence of Yod1(C160S), RI_{332} is arrested at the ER membrane (*5th to 8th lanes*). In the presence of EBV protease, polyubiquitin chains are preemptively removed, and RI_{332} is arrested either at the ER membrane or in the cytosol. At the higher time point, deglycosylated RI_{332} appears in the cytosolic fraction indicating dislocation of the substrate from the ER to the cytosol and stabilization (*9th to 12th lanes*). Semi-intact cells transfected with EBV and RI_{332} were incubated in the presence of either trypsin (*tryp*) alone (*13th to 16th lanes*) or with trypsin pretreated with trypsin inhibitor (*17th to 20th lanes*), for 10 min at 37 °C. Deglycosylated RI_{332} is proteolyzed in the presence of added trypsin, verifying its cytosolic orientation, although it remains protected when proteolytic activity of trypsin is blocked by pretreating with an inhibitor. Images are representative of experiments performed at least twice. *B,* TCRα is dislocated to the cytosol and degraded at the proteasome in semi-intact cells. HEK293T cells transfected with TCRα were permeabilized with PFO to separate supernatant and pellet. Fully glycosylated TCRα appeared in the pellet fraction, and deglycosylated TCRα appeared in the supernatant, indicating dislocation from the ER to the cytosol. Extraction of deglycosylated TCRα into the cytosol remains unaffected in the presence or absence of 0.5 M NaCl.

Similarly, the T cell receptor αsubunit (TCRα), a membrane-bound glycoprotein, is retained in the ER and destroyed when expressed in the absence of its subunits required for proper assembly, which involves dislocation, progressive deglycosylation, and proteasomal proteolysis (16). Using PFO as a tool to fractionate cytosol from subcellular organelles, we could capture deglycosylated TCRα in the supernatant fraction when transfected with EBV-DUB (Fig. 3*B*). In HEK293T cells that express TCRα and EBV-DUB, deglycosylated TCRα appeared in the cytosol after 3 h of chase (both in the presence and absence of high salt), as evident from its partitioning (Fig. 3*B, 5th to 12th lanes*) into the supernatant upon PFO-mediated fractionation. This observation is in contrast to deglycosylated RI_{332}, which shows a greater tendency of associating with the membrane and requires addition of 0.5 M NaCl for the most efficient extraction into the supernatant fraction.

Dislocation of Misfolded Proteins Is Restored in Permeabilized Cells through Exogenous Addition of Purified EBV-DUB—In cells that express Yod1C160S, fully glycosylated RI_{332} accumulates in the ER lumen because dislocation is blocked (15). We hypothesize that this arrest is due to the inability of ubiquitylated RI_{332} to be extracted and instead causes an obstruction in the dislocon. Can addition of purified exogenous EBV-

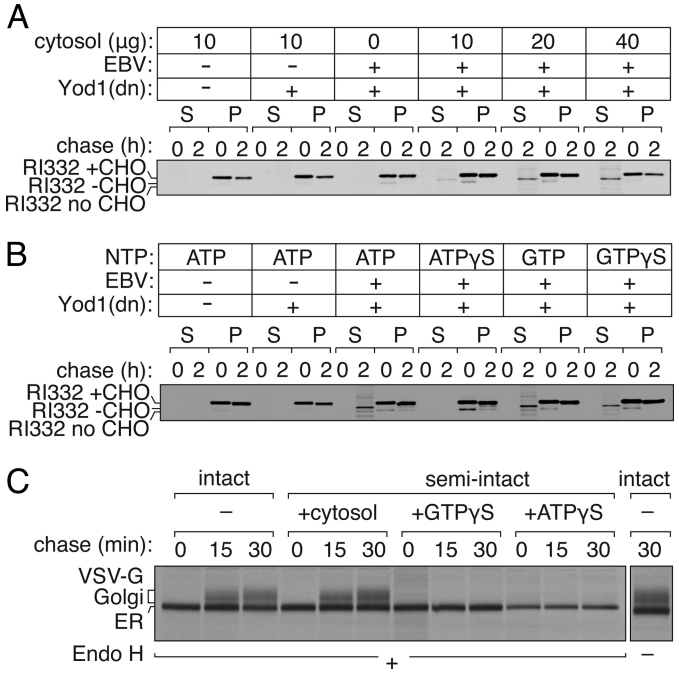

FIGURE 4. **Dislocation of substrates is restored in semi-intact cells through exogenous addition of EBV-DUB.** *A,* cytosol dependence of substrate dislocation after EBV addition. HEK293T cells were transfected with RI_{332} and Yod1(C160S). Control cells were transfected with pcDNA. Cells were pulse-labeled with [^{35}S]cysteine/methionine, permeabilized, and incubated with 10 μg of EBV and varying amounts of cytosol (0, 10, 20, or 40 μg) in Hanks' buffer at 37 °C. At 0 and 90 min, aliquots were withdrawn, and supernatant (*S*) and pellet (*P*) fractions were separated by centrifugation and probed by SDS-PAGE and autoradiography. *B,* HEK293T cells transfected with RI_{332} were radiolabeled, permeabilized, and incubated with EBV and cytosol supplemented with ATP (1 mM), ATPγS (1 mM), GTP (1 mM), or GTPγS (1 mM). Supernatant and pellet fractions were probed for dislocated RI_{332}. *C,* in PFO-permeabilized HEK293T cells, the secretory pathway remains functional and sensitive to GTPγS. HEK293T cells transfected with VSV-G were pulsed with [^{35}S]cysteine/methionine, PFO-permeabilized, and chased with cytosol for 0, 15, and 30 min in the presence of concentrated cytosol (*4th to 6th lanes*) or cytosol supplemented with either GTPγS (*7th to 9th lanes*) or ATPγS (*10th to 12th lanes*). At every time point, VSV-G was recovered from lysates by immunoprecipitation on chicken VSV-G antibody, digested with endoglycosidase H (*Endo H*), and resolved by SDS-PAGE. Trafficking of VSV-G in intact cells was monitored in parallel (*1st to 3rd lanes*).

DUB to these semi-intact cells jump-start dislocation of RI_{332} through removal of Ub from the RI_{332} intermediate stalled at the ER? We used PFO to permeabilize HEK293T cells that co-express RI_{332} and Yod1C160S, and we did so in the presence of purified EBV-DUB, delivered to the cytoplasm by means of a transient mild hypotonic shock. Residual cytosol was removed from these semi-intact cells by washing with buffer. To resume dislocation, the reaction mixture was supplemented with concentrated HEK293T cytosol (40 μg of total protein) and ATP (1 mM). Incubation of PFO-perforated cells with EBV-DUB in the absence of added cytosol fails to restore dislocation of RI_{332} from the ER; no product appears in the supernatant fractions (Fig. 4*A, 1st to 12th lanes*). Addition of 10 – 40 μg (total protein) of cytosol (5 mg/ml) together with EBV-DUB allows dislocation of RI_{332} to resume. Cytosolic components are therefore essential to facilitate the process. Our data suggest the following. In the presence of Yod1C160S, a very minor fraction (beyond the limit of detection by our biochemical methods) of membrane-bound RI_{332} retains its ubiquitylated status, blocking any further association of luminally oriented RI_{332} with the E3 ubiquitin ligase. As a consequence, most RI_{332} remains confined to the lumen of the ER in its glycosylated form. The lack of detectable ubiquitylated RI_{332} in the autoradiograms is suggestive of a very minor fraction of ubiquitylated substrate responsible for stalling further dislocation; we know of no deubiquitylating enzymes that reside within the ER lumen that could reverse ubiquitylation. Upon addition of exogenous EBV-DUB, this fraction is deubiquitylated and reaches the cytoplasm, allowing continued dislocation of the luminally positioned substrate. Appearance of a significantly larger fraction of deglycosylated RI_{332} (easily visualized by autoradiography) suggests that the rate of ubiquitylation by the E3 ligase is comparable with that of deubiquitylation by EBV-DUB, allowing continuous passage of RI_{332} from the ER lumen to the cytosol. This experiment demonstrates the feasibility of jump-starting, in a synchronized manner, the dislocation reaction.

Transport of misfolded proteins from the ER to the cytosol requires ATP, as inferred from the involvement of p97, a AAA-ATPase. To examine more directly the NTP requirement in the process of dislocation of RI_{332} in PFO-perforated cells, we added either ATP, GTP, or their nonhydrolyzable analogs. Addition of ATP allowed dislocation of RI_{332} to proceed, whereas the inclusion of ATPγS blocked it (Fig. 4*B, 9th to 16th lanes*). Presence of either GTP or GTPγS did not affect dislocation (Fig. 4*B, 17th to 24th lanes*). In contrast to the process of dislocation, transport along the secretory pathway in semi-intact cells remained GTP-sensitive. As a positive control for the ability of GTPγS to block a trafficking step in PFO-perforated cells, we monitored transport of VSV-G from the ER to the Golgi in semi-intact cells, based on acquisition of complex glycan modifications (Fig. 4*C*). As read-out, we followed the conversion of *N*-linked oligosaccharides on VSV-G from their high mannose endoglycosidase H-sensitive precursors to terminally glycosylated, mature Golgi forms, resistant to endoglycosidase H digestion. We compared kinetics of VSV-G trafficking in intact cells with that in PFO-permeabilized semi-intact cells (Fig. 4*C*). Transport of VSV-G through the Golgi was greatly diminished in semi-intact cells in the absence of cytosol, which is evident from its sensitivity to endoglycosidase H digestion.[4] When compared with intact cells, we achieved near-complete recovery of VSV-G maturation in semi-intact cells when supplemented with concentrated cytosol. We observed inhibition of transport of VSV-G in semi-intact cells when cytosol was supplemented with GTPγS. Transport through the secretory pathway thus requires GTP hydrolysis (27, 28), whereas dislocation of misfolded proteins does not.

Efficiency of EBV Add-back Increases with Decreasing Buffer Osmolarity and Increase in EBV-DUB Concentration—Dislocation of RI_{332} in semi-intact cells upon addition of purified EBV-DUB increases with the amount of cytosol added (Fig. 4*A*). To optimize conditions and improve delivery of macromolecules to semi-intact cells, we tested increasing concentrations of EBV-DUB and decreasing osmolarity of the permeabilization buffer. We reduced ionic strength to achieve a greater osmotic differential and so improve delivery of EBV-DUB to semi-intact cells. As anticipated, by increasing the amount of purified EBV-DUB supplied, we observed a dose-dependent increase in the amount of dislocated intermediate (Fig. 5, *A* and *B*). Similarly,

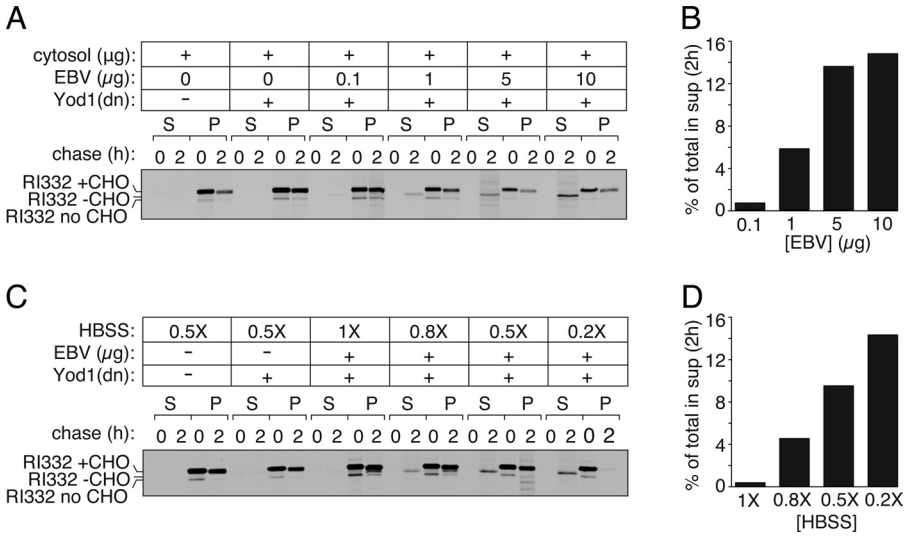

FIGURE 5. **Characterization of purified EBV delivery to semi-intact cells.** *A,* dose-dependent EBV delivery to semi-intact cells. HEK293T cells were transfected with RI_{332} and Yod1 (C160S) to stall dislocation in the ER. Semi-intact cells prepared with PFO were incubated with 40 μg of cytosol, 1 mM ATP, and varying amounts of EBV to monitor dose dependence of RI_{332} export from the ER. In parallel, one set of control cells received only RI_{332}. Another set of control cells received RI_{332} and Yod1(C160S) and were incubated with a mock reaction mixture without EBV present. *B,* quantitation of the autoradiogram shown in *A*. *Graphs* represent the amount of radioactivity in the supernatant fractions at 2 h as a fraction of total radioactivity in the supernatant (*S*) and pellet (*P*) fractions. *C,* dependence of EBV delivery to semi-intact cells on buffer osmolarity. HEK293T cells transfected with RI_{332} and Yod1 were permeabilized using PFO. Semi-intact cells were incubated in 10 μg of purified EBV, 1 mM ATP, and 40 μg of cytosol in Hanks' buffer of 1, 0.8, 0.5, or 0.2× ionic strength, respectively, to provide a greater hypotonic shock for better EBV delivery to semi-intact cells. *D,* quantitation of the autoradiogram shown in *C*. All experiments were performed at least twice.

by reducing osmolarity from 1 to 0.2× Hanks' buffer equivalent to modulate delivery of EBV-DUB, we observed an increase in the amount of deglycosylated intermediate that appeared in the cytosolic fraction (Fig. 5, *C* and *D*).

Exogenous Addition of EBV-DUB Stabilizes Class I MHC and TCRα in Semi-intact Cells—To extend our findings to substrates beyond RI_{332}, we monitored export and degradation of TCRα chain in HEK293T cells (Fig. 6*A*). TCRα is a glycoprotein in which four *N*-glycosylation sequons are used; when expressed in HEK293T cells, TCRα is degraded by the UPS (16, 29). Cells co-expressing TCRα and Yod1C160S were pulse-labeled with [^{35}S]cysteine/methionine, permeabilized with PFO, and exposed to exogenously added EBV-DUB in the presence and absence of additional cytosol. In the presence of added EBV-DUB and cytosol, deglycosylated TCRα appeared in the supernatant fraction at the 3-h time point, indicating that transport had resumed with concomitant stabilization of dislocated TCRα. We observed the appearance of a minor fraction of deglycosylated TCRα in the absence of added ATP and cytosol, possibly due to residual cytosol, despite permeabilization. Supplementing the reaction mixture with concentrated cytosol and ATP significantly improved recovery of cytosolic deglycosylated TCRα, as also seen for RI_{332}.

In astrocytoma cells that express HCMV US11, class I MHC molecules are rapidly degraded by the UPS (18, 30). PFO-permeabilized US11-expressing cells supported rapid degradation of class I molecules when supplemented with ATP and cytosol (Fig. 6*B, 1st to 6th lanes*). To test the effect of EBV-DUB on MHC class I degradation, we created PFO-mediated semi-intact cells to supply purified EBV-DUB. US11-expressing astrocytomas proved difficult to transiently transfect with Yod1C160S due to poor transfection efficiency. However, addition of EBV-DUB to these semi-intact cells almost completely

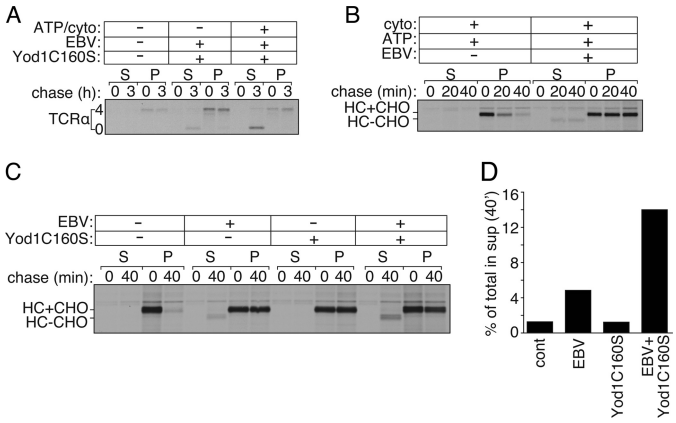

FIGURE 6. **TCRα and class I MHC dislocation measured in semi-intact cells.** *A,* HEK293T cells transfected with TCRα and Yod1 (C160S) were pulsed with [^{35}S]cysteine/methionine, permeabilized using PFO, and incubated with purified EBV supplemented with 40 μg of cytosol (*cyto*) and 1 mM ATP. *B,* astrocytoma cells stably transfected with HCMV US11 were pulsed with [^{35}S]cysteine/methionine, permeabilized using PFO, and incubated with 40 μg of cytosol and 1 mM ATP for 0, 20, and 40 min in the absence or presence of purified EBV. *C,* US-11 expressing astrocytomas were stably transfected with either WTYod1 or Yod1C160S. Cells were radiolabeled, followed by PFO permeabilization to supply concentrated cytosol in the presence of absence of purified EBV for 0 and 40 min. *D,* quantitation of the autoradiogram shown in *C*. *Graphs* represent the amount of radioactivity in the supernatant fractions at 40 min as a fraction of total radioactivity present in the supernatant (*S*) and pellet (*P*) fractions. Images are representative of experiments performed twice.

arrested fully glycosylated MHC-I in the ER, with the appearance of a minor fraction of deglycosylated MHC-I in the cytosolic fractions at the 20- and 40-min time points (Fig. 6*B, 7th to 12th lanes*). Ubiquitylation of class I molecules must therefore be a rate-limiting step in this case, contrary to what we observe for RI_{332}. We surmise that addition of EBV-DUB rapidly removes polyubiquitin chains from MHC class I, at a rate faster than re-ubiquitylation and subsequent recruitment of the dis-

location components. The net result is that the reaction stalls. In cells that co-express US11 and Yod1C160S, class I MHC products would be positioned such that further addition of EBV-DUB would allow a greater fraction of the substrate to arrive in the cytosol and be deubiquitylated and deglycosylated. To test our hypothesis, we generated a cell line that stably expresses US11 with either Yod1C160S or Yod1WT, as confirmed by immunoblotting. These cells were pulse-labeled with [^{35}S]cysteine/methionine, followed by PFO treatment to form semi-intact cells. EBV-DUB was supplied to these semi-intact cells and incubated with concentrated cytosol for 0 and 40 min (Fig. 6*C*). At each time point, cells were separated into supernatant and pellet fractions. In the presence of Yod1WT with no EBV-DUB added, class I MHC is degraded rapidly as expected. When these cells express Yod1C160S, class I MHC remains stable in its glycosylated form in the ER (Fig. 6*C, 5th to 8th lanes*). Although semi-intact cells supplied with EBV-DUB show a near complete stabilization of class I in the ER, with a minor fraction appearing in the cytosol, addition of EBV-DUB to cells that stably express Yod1C160S leads to a greater fraction of class I in the cytosol in its deglycosylated form (Fig. 6*D*). This observation supports our hypothesis that the presence of Yod1C160S positions the substrate in its ubiquitylated state at the ER, such that the downstream dislocation components are in place for extraction to the cytosol to occur. Consequently, addition of EBV-DUB to these cells results in a larger fraction of the substrate to appear in the cytosol. These data are strongly suggestive of distinct modes of E3 ubiquitin ligase involvement in the pathway of RI_{332} and MHC-I dislocation.

Dislocation Substrates Are Polyubiquitylated in the Presence of Yod1C160S—We blocked dislocation of misfolded substrates in the ER by expression of Yod1C160S, causing accumulation of glycosylated RI_{332}. As proposed in the model, we hypothesize that this stabilization is due to stalled dislocation, because of occlusion of ubiquitylated RI_{332} from the central pore of p97 or of any other endogenous substrate that might require dislocation via this pathway. Purified EBV-DUB supplied to semi-intact cells overcomes this blockade and restores dislocation. Detecting ubiquitylated substrate intermediates in autoradiograms has been challenging, possibly due to low levels and inherent instability of such intermediates. In an alternative approach, we transiently transfected HEK293T cells with untagged RI_{332}, Yod1C160S, and either empty control plasmid or HA-Ub (Fig. 7). We permeabilized cells with PFO and supplied purified EBV-DUB to allow release of stalled RI_{332} from the ER. After incubating with EBV-DUB for 60 min, samples were solubilized in Nonidet P-40 lysis buffer in the presence of 5 mg/ml *N*-ethylmaleimide to block endogenous DUB activities during lysis and immunoprecipitated RI_{332} with anti-ribophorin antibodies. Eluted samples were then resolved on SDS-PAGE and immunoblotted with anti-HA antibodies. In cells that express Yod1C160S and HA-Ub, a smear of polyubiquitylated RI_{332} was detected in the immunoprecipitated sample. When exogenous EBV was added back to these permeabilized cells, ubiquitylated intermediates disappeared, indicating substrate de-ubiquitylation. Upon separating the cytosol and the pellet fractions, deglycosylated RI_{332} appeared in the cytosol and glycosylated RI_{332} remained in the pellet fraction. In parallel, in cells expressing WTYod1 treated with ZL3VS to block proteasomal activity, polyubiquitylated RI332 appeared in both the cytosolic and pellet fractions. These data, in conjunction with pulse-chase assays, support our proposed model that dislocation substrates remain ubiquitylated in the presence of Yod1C160S, causing them to accumulate at the ER membrane. Yod1C160S prevents dislocation not only of the substrates introduced by transfection but presumably other endogenous proteins destined for dislocation. Although we can demonstrate the presence of ubiquitylated RI_{332} in cells that express Yod1C160S, it is unlikely to be the only ubiquitylated substrate that could contribute to occlusion of the dislocation machinery. Regardless, inclusion of EBV-DUB removes Ub from RI_{332}, a reaction that coincides with the initiation of dislocation.

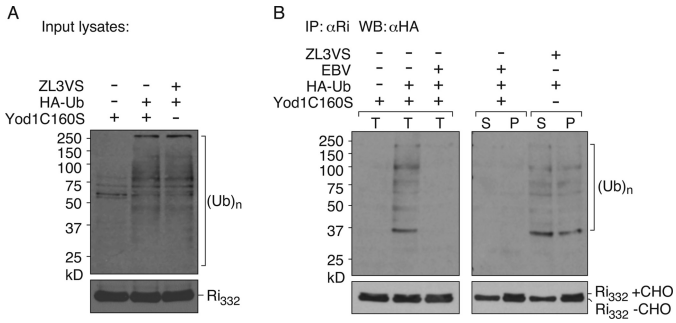

FIGURE 7. **Polyubiquitylation of a dislocation substrate prior to degradation.** HEK293T cells were transfected with RI_{332}, Yod1C160S, and empty vector or HA-Ub. Cells were permeabilized with 100 nM PFO and incubated with purified EBV in 0.5× HBSS. After 60 min of incubation, samples were either directly solubilized in buffer containing 0.5% Nonidet P-40 supplemented with 5 mg/ml *N*-ethylmaleimide or supernatant and pellet fractions were first separated by centrifugation followed by dilution/lysis. RI_{332} was immunoprecipitated on protein A beads coupled to anti-RI antibodies; eluates were resolved by SDS-PAGE, and polyubiquitylated material was visualized by anti-HA. In parallel, cells transfected with RI_{332} and HA-Ub were treated with 20 μM ZL3VS to inhibit the proteasome. Cells were permeabilized using PFO and separated into cytosolic and pellet components. RI_{332} was immunoprecipitated from both fractions, and eluates were resolved by SDS-PAGE and visualized using anti-HA antibodies. *A,* lysates from cells expressing RI_{332}, empty vector, or HA-Ub, −/+ Yod1C160S and −/+ ZL3VS were directly immunoblotted and probed with anti-HA for ubiquitin levels and anti-RI for RI_{332} levels. *B, left panel,* semi-intact cells expressing Yod1C160S, RI_{332} and empty vector/HA-Ub were incubated with −/+ 1 μg of purified EBV. After 60 min, reaction was terminated by lysis in 0.5% Nonidet P-40 lysis buffer and immunoprecipitated (*IP*) with anti-RI antibodies. The eluates were visualized by immunoblotting with anti-HA antibodies. *T,* total. *Right panel,* after 60 min of incubation with EBV or ZL3VS, cells were first separated into cytosol and pellet fractions and immunoprecipitated with anti-RI antibodies, and eluates were visualized by immunoblotting with anti-HA antibodies. Immunoisolated material was also probed with anti-RI antibodies for RI_{332} levels. *S,* supernatant (cytosol), *P,* pellet. Images are representative of experiments performed three times.

DISCUSSION

Using a number of reporters with distinct physical properties (RI_{332}, TCRα, and MHC-I), we show that dislocation in semi-intact cells requires ATP and cytosol, confirming and extending our earlier data for MHC-I in digitonin-permeabilized cells (30). Unlike protein trafficking through the secretory pathway, dislocation of substrates from the ER was insensitive to the inclusion of GTPγS. We had proposed earlier that deubiquitylation of substrates designated for proteasomal degradation is a necessary step for dislocation from the ER. If correct, two rounds of ubiquitylation would be required for dislocation and degradation of RI_{332} as follows: an initial round at the ER mem-

brane to engage the p97 complex, followed by deubiquitylation, and a second round of ubiquitylation in the cytosol to tag substrates for proteasomal degradation. Ubiquitylation at the ER membrane appears to be more essential for recognition by downstream effectors than for providing a handle for generating a mechanical force for substrate passage through the p97 complex (31). Data presented here with multiple substrates confirm this model of protein dislocation.

We provide a key mechanistic insight in the dislocation reaction that clears misfolded proteins from the ER. We find that expression of Yod1C160S, a dominant negative version of an ER-associated deubiquitylase, impedes dislocation through the accumulation of a ubiquitylated intermediate. Through delivery of a heterologous deubiquitylase in a semi-intact cell preparation, we can relieve this inhibition and jump-start the dislocation reaction. The level to which the stalled intermediate accumulates is such that we cannot detect biochemically the presence of the ubiquitylated species, yet the consequences of providing an exogenous active deubiquitylase, EBV-DUB, is compelling evidence that even these small amounts of the ubiquitylated intermediate must be sufficient to occlude the dislocon and halt the transfer of proteins across the membrane.

Intracellular transport of proteins in a cell-free system requires that events observed *in vitro* faithfully recapitulate the process occurring *in vivo*. Although methods based on subcellular fractionation or detergent-solubilized crude extracts have provided important information regarding intracellular protein trafficking, limitations include the disruption of essential cellular architecture in the course of homogenization or cell lysis. Semi-intact cells, from which segments of the plasma membrane have been selectively removed, retain the necessary subcellular integrity essential for intracellular transport to proceed. Such systems allow access of otherwise cell-impermeant macromolecules to the cytoplasmic side and so enable mechanistic analyses related to a pathway.

Here, we use PFO, a cholesterol-dependent bacterial pore-forming toxin, to perforate the plasma membrane under mild physiological conditions and monitor protein dislocation from their initial ER localization to the cytosol. The PFO-based assay provides a level of precision and sensitivity that we have been unable to match in microsome preparations or other available strategies. The assay reports on intracellular transport of proteins with minimal damage to subcellular organelles. We observed efficient protein trafficking along the secretory pathway as monitored through VSV-G and HA transport when compared with intact cells. Furthermore, we could readily monitor dislocation of glycoproteins from the ER to the cytosol, and we obtained clean separation of ER-resident (glycosylated) and cytoplasmic (deglycosylated) substrates. We had comparatively limited success in measuring dislocation of class I MHC products in US11/US2-expressing cells (32) and for this reason developed the PFO-based alternative to the microsome-based system. Digitonin-based semi-intact cell systems in our hands also perform less robustly than the PFO system described here. Treatment with PFO is largely directed and confined to the plasma membrane, conferring little to no perturbation of the integrity of the ER membrane. Given the involvement of a variety of membrane-integral and membrane-tethered proteins that must connect to cytoplasmic components to carry out the entire dislocation and degradation pathway (22), minimal disruption of cellular architecture appears to be a prerequisite to observe these reactions in semi-intact cells.

Acknowledgments—We are grateful to R. Ernst for purified EBV-DUB; Art Johnson for the plasmid encoding perfringolysin O; Lee Kim Swee for help with figures, and all the Ploegh laboratory members for helpful discussions and suggestions.

REFERENCES

1. Park, E., and Rapoport, T. A. (2012) Mechanisms of Sec61/SecY-mediated protein translocation across membranes. *Annu. Rev. Biophys.* **41,** 21–40
2. Braakman, I., and Bulleid, N. J. (2011) Protein folding and modification in the mammalian endoplasmic reticulum. *Annu. Rev. Biochem.* **80,** 71–99
3. Carvalho, P., Stanley, A. M., and Rapoport, T. A. (2010) Retrotranslocation of a misfolded luminal ER protein by the ubiquitin-ligase Hrd1p. *Cell* **143,** 579–591
4. Scott, D. C., and Schekman, R. (2008) Role of Sec61p in the ER-associated degradation of short lived transmembrane proteins. *J. Cell Biol.* **181,** 1095–1105
5. Ye, Y., Shibata, Y., Yun, C., Ron, D., and Rapoport, T. A. (2004) A membrane protein complex mediates retro-translocation from the ER lumen into the cytosol. *Nature* **429,** 841–847
6. Lilley, B. N., and Ploegh, H. L. (2004) A membrane protein required for dislocation of misfolded proteins from the ER. *Nature* **429,** 834–840
7. Ploegh, H. L. (2007) A lipid-based model for the creation of an escape hatch from the endoplasmic reticulum. *Nature* **448,** 435–438
8. Olzmann, J. A., and Kopito, R. R. (2011) Lipid droplet formation is dispensable for endoplasmic reticulum-associated degradation. *J. Biol. Chem.* **286,** 27872–27874
9. Claessen, J. H., Kundrat, L., and Ploegh, H. L. (2012) Protein quality control in the ER. Balancing the ubiquitin checkbook. *Trends Cell Biol.* **22,** 22–32
10. Smith, M. H., Ploegh, H. L., and Weissman, J. S. (2011) Road to ruin. Targeting proteins for degradation in the endoplasmic reticulum. *Science* **334,** 1086–1090
11. Reyes-Turcu, F. E., Ventii, K. H., and Wilkinson, K. D. (2009) Regulation and cellular roles of ubiquitin-specific deubiquitinating enzymes. *Annu. Rev. Biochem.* **78,** 363–397
12. Mueller, B., Klemm, E. J., Spooner, E., Claessen, J. H., and Ploegh, H. L. (2008) SEL1L nucleates a protein complex required for dislocation of misfolded glycoproteins. *Proc. Natl. Acad. Sci. U.S.A.* **105,** 12325–12330
13. Ernst, R., Mueller, B., Ploegh, H. L., and Schlieker, C. (2009) The otubain YOD1 is a deubiquitinating enzyme that associates with p97 to facilitate protein dislocation from the ER. *Mol. Cell* **36,** 28–38
14. Claessen, J. H., Mueller, B., Spooner, E., Pivorunas, V. L., and Ploegh, H. L. (2010) The transmembrane segment of a tail-anchored protein determines its degradative fate through dislocation from the endoplasmic reticulum. *J. Biol. Chem.* **285,** 20732–20739
15. Ernst, R., Claessen, J. H., Mueller, B., Sanyal, S., Spooner, E., van der Veen, A. G., Kirak, O., Schlieker, C. D., Weihofen, W. A., and Ploegh, H. L. (2011) Enzymatic blockade of the ubiquitin-proteasome pathway. *PLoS Biol.* **8,** e1000605
16. Huppa, J. B., and Ploegh, H. L. (1997) The α chain of the T cell antigen receptor is degraded in the cytosol. *Immunity* **7,** 113–122
17. Flanagan, J. J., Tweten, R. K., Johnson, A. E., and Heuck, A. P. (2009) Cholesterol exposure at the membrane surface is necessary and sufficient to trigger perfringolysin O binding. *Biochemistry* **48,** 3977–3987
18. Wiertz, E. J., Jones, T. R., Sun, L., Bogyo, M., Geuze, H. J., and Ploegh, H. L. (1996) The human cytomegalovirus US11 gene product dislocates MHC class I heavy chains from the endoplasmic reticulum to the cytosol. *Cell* **84,** 769–779
19. Misaghi, S., Pacold, M. E., Blom, D., Ploegh, H. L., and Korbel, G. A. (2004) Using a small molecule inhibitor of peptide. *N*-Glycanase to probe its role

in glycoprotein turnover. *Chem. Biol.* **11,** 1677–1687
20. Shatursky, O., Heuck, A. P., Shepard, L. A., Rossjohn, J., Parker, M. W., Johnson, A. E., and Tweten, R. K. (1999) The mechanism of membrane insertion for a cholesterol-dependent cytolysin. A novel paradigm for pore-forming toxins. *Cell* **99,** 293–299
21. Walev, I., Bhakdi, S. C., Hofmann, F., Djonder, N., Valeva, A., Aktories, K., and Bhakdi, S. (2001) Delivery of proteins into living cells by reversible membrane permeabilization with streptolysin-O. *Proc. Natl. Acad. Sci. U.S.A.* **98,** 3185–3190
22. Beckers, C. J., Keller, D. S., and Balch, W. E. (1987) Semi-intact cells permeable to macromolecules. Use in reconstitution of protein transport from the endoplasmic reticulum to the Golgi complex. *Cell* **50,** 523–534
23. Ikonen, E., Tagaya, M., Ullrich, O., Montecucco, C., and Simons, K. (1995) Different requirements for NSF, SNAP, and Rab proteins in apical and basolateral transport in MDCK cells. *Cell* **81,** 571–580
24. Nelson, L. D., Chiantia, S., and London, E. (2010) Perfringolysin O association with ordered lipid domains. Implications for transmembrane protein raft affinity. *Biophys. J.* **99,** 3255–3263
25. de Virgilio, M., Weninger, H., and Ivessa, N. E. (1998) Ubiquitination is required for the retro-translocation of a short lived luminal endoplasmic reticulum glycoprotein to the cytosol for degradation by the proteasome. *J. Biol. Chem.* **273,** 9734–9743
26. Mueller, B., Lilley, B. N., and Ploegh, H. L. (2006) SEL1L, the homologue of yeast Hrd3p, is involved in protein dislocation from the mammalian ER. *J. Cell Biol.* **175,** 261–270
27. Balch, W. E. (1990) Small GTP-binding proteins in vesicular transport. *Trends Biochem. Sci.* **15,** 473–477
28. Symons, M., and Rusk, N. (2003) Control of vesicular trafficking by Rho GTPases. *Curr. Biol.* **13,** R409–R418
29. Yu, H., Kaung, G., Kobayashi, S., and Kopito, R. R. (1997) Cytosolic degradation of T-cell receptor α chains by the proteasome. *J. Biol. Chem.* **272,** 20800–20804
30. Shamu, C. E., Story, C. M., Rapoport, T. A., and Ploegh, H. L. (1999) The pathway of US11-dependent degradation of MHC class I heavy chains involves a ubiquitin-conjugated intermediate. *J. Cell Biol.* **147,** 45–58
31. Ye, Y., Meyer, H. H., and Rapoport, T. A. (2003) Function of the p97-Ufd1-Npl4 complex in retrotranslocation from the ER to the cytosol. Dual recognition of nonubiquitinated polypeptide segments and polyubiquitin chains. *J. Cell Biol.* **162,** 71–84
32. Furman, M. H., Ploegh, H. L., and Tortorella, D. (2002) Membrane-specific, host-derived factors are required for US2- and US11-mediated degradation of major histocompatibility complex class I molecules. *J. Biol. Chem.* **277,** 3258–3267